# Analysis of the ICE Model

**Anupam Prasad Vedurmudi**


München 2013

# Analysis of the ICE Model

**Anupam Prasad Vedurmudi**

Dissertation
an der Fakultät für Physik
der Ludwig–Maximilians–Universität
München

vorgelegt von
Anupam Prasad Vedurmudi
aus Kolkata, Indien

München, den June 2, 2013

Erstgutachter: Prof. Dr. J. Leo van Hemmen
Zweitgutachter: Zweitgutachter
Tag der mündlichen Prüfung: Prüfungsdatum

# Contents

# List of Figures

# List of Tables

# Abstract

Hier steht eine maximal einseitige Zusammenfassung der Dissertation.

Dies ist ein neuer Absatz.

# Chapter 1

# Introduction

# Chapter 2

# The ICE Model

Several terrestrial vertebrates, e.g. lizards, frogs, alligators and many birds, possess a hearing mechanism very different to that of mammals: their tympanic membranes are coupled through large eustachian tubes and a large mouth cavity resulting in the influence of the vibrations of one tympanic membrane on those of the other. This is illustrated in 2.1. The typically small head sizes (compared to sound wavelength) of these animals result in small phase differences (ITDs) and negligible amplitude difference (ILDs) between the ears. The coupling serves to enhance the ITDs and create ILDs between the tympanal vibrations. These differences show directionality and serve as hearing cues for localization.

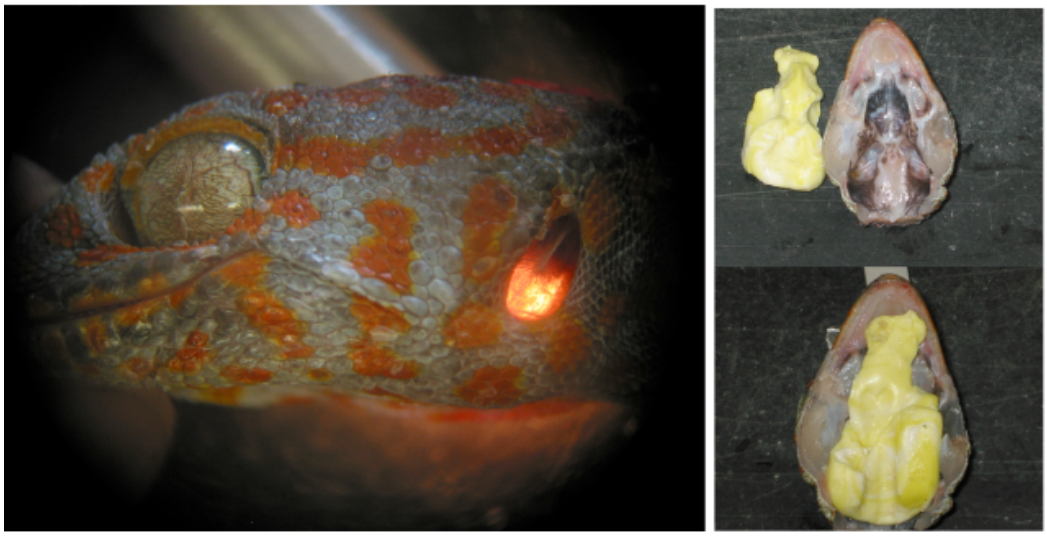

Figure 2.1: Left: Picture of a Tokay gecko's head with the snout pointing to the left. The tympanic membrane is illuminated from behind by a light source on the other side of the head. The cartileginous extracolumella can be seen attached to the upper part of the membrane. Right: Cast imprint of the mouth cavity of the gecko with the snout pointing to the top. The figures illustrate the coupling of the tympani through the mouth cavity. Photographs courtesy of Jakob Christensen-Dalsgaard.

In this chapter we present a model for the middle-ear of lizards - specifically the Tokay Gecko and the Common House Gecko. Our goal is to do this in the simplest possible way while ensuring an accurate reproduction of its main properties. The main components of such a system are the mouth-cavity, the two tympani and the two *extracolumella* (one on each tympanum). In general, the shape of the mouth-cavity is highly irregular and therefore not conducive to an analytical treatment. Moreover, the system corresponds to a pair of coupled second-order PDE's with moving boundaries. For this reason we will need to make further approximations for the sake of expediency.

In order to make the system more analytically tractable we will, as before, study a geometry in which a pair of sectoral membranes are coupled through a cylindrical cavity. The cylindrical geometry allows an accurate calculation of the pressure distribution inside the cavity at both low and high frequencies. By accounting for the presence of the asymetrically attached extracolumella, we will also explain the complex vibration patterns of the membrane. At the end of this chapter, we will have the expressions that describe the steady-state vibrations of both eardrums as a function direction and frequency.

## 2.1 Description of the Model

In order to describe the ICE model, we first need to list its basic components and justify their properties based on a realistic mouth cavity.

In Sec. 2.1.1, we will describe the cylindrical model for the mouth cavity and state the reasons for our choice of the geometry and the dimensions used. We will then proceed to describe the middle ear system and its main components of interest, the *extracolumella* and the *tympani* in Sec. 2.1.2. Finally, in Sec. 2.1.3 we will analyse the dependence of the acoustic input to both eardrums on the direction of the sound source, head size and shape.

### 2.1.1 Mouth Cavity

In the earlier treatment of the ICE model, the mouth canal is modelled as a simple cylinder closed at both ends by rigidly clamped (baffled) circular membranes; these model the tympanic membranes. As shown by Vossen in [1, p. 21] and [2], the length of the cylinder was chosen to be equal to the interaural distance and the radius of the model tympanum is determined from the typical area of the realistic tympanum. The advantage of using a cylindrical cavity model for the mouth cavity is that the pressure distribution inside the cavity is easy to calculate. The pressure distribution inside the cavity becomes highly non-uniform with increasing frequency and a cylindrical cavity simplifies its calculation.

On the other hand, in this description the small area of the tympani results in a cavity volume which is an order of magnitude smaller than that of the realistic mouth-cavity in the corresponding animal. In general, a smaller volume results in a stronger coupling - both in terms of an increased iTD and an increased iLD. For this reason, the earlier model overestimates the iTDs and iLDs at low and high frequencies respectively.

In order to get around this problem we make some slight modifications to the model. Essentially, we maintain the cylindrical shape of the internal cavity but require it to have a volume which is equal to that of the realistic cavity ($V_{cav}$). We also maintain the same tympanum size and interaural distance and can therefore calculate the radius of the cylinder as,

$$a_{cyl} = \sqrt{\frac{V_{cav}}{\pi L}} \tag{2.1}$$

where $a_{cyl}$ is the cylinder radius and $L$ is the interaural distance. Simply put, the model

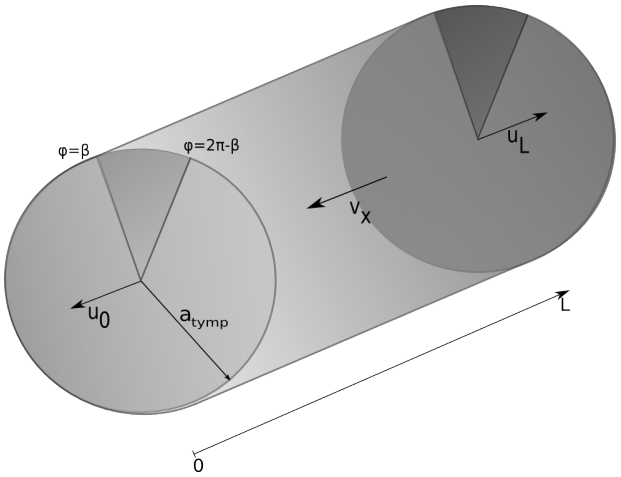


(a) The previous geometric reprentation of the ICE model.

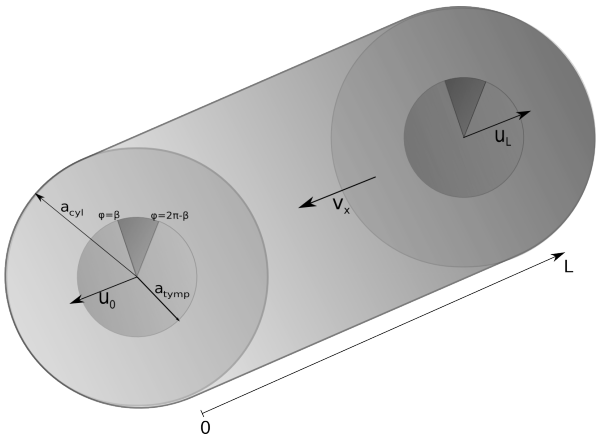


(b) The representation of the new model.

Figure 2.2: The bold arrows represent the direction conventions along the cylinder's axis. The new model is represented by a cylinder of radius $a_{cyl}$ and length $L$ closed at both ends by sectoral membrane of radius $a_{tymp}$. The darkly shaded region corresponds to the extracolumella (described in Sec. 2.1.2).

consists of a cylindrical shell of radius $a_{cyl}$ and length $L$ with circular holes on either side

with the radius of the tympanic membrane, $a_{tymp}$. These holes are in turn closed by rigidly clamped membranes which will be described in the next section. The previous and current geometric representations of our model are shown in figures 2.2a and 2.2b. The darkly shaded circular surfaces in fig. 2.2b at ends 0 and $L$ correspond to the two eardrums.

We will be working with the cylindrical polar coordinates, $(r, \phi, x)$. The direction along the cylindrical axis is denoted by $x$ and $(r, \phi)$ are the polar coordinates of the plane perpendular to the $x$-direction. Directions outward from the cylinder are taken as positive (in $x$) and those inward are taken as negative.

### 2.1.2 Middle Ear

The main components of the middle-ear of lizards are the two eardrums, the columella and the two cartileginous extracolumella. The tympanic membrane or the eardrum is a thin membrane that separates the outer ear and the middle ear and vibrates in response to external sound waves. Unlike humans, lizards possess only a single middle ear bone, the *columella*, that is connected to both eardrums by means of a cartileginous element, the *extracolumella*.

The membrane-extracolumella-columella system functions as a second-order lever where the membrane - driven by the internal and external pressures - causes a displacement of the extension of the extracolumella (known as the inferior process). This motion is in turn transmitted via the columella and columellar footplate to the inner ear (cochlea). The inner-ear translates this motion into electrochemical impulses which will be passed on to the brain via the auditory nerve. The columella-extracolumella system effectively transmits the mechanical vibrations from the eardrums to the inner ear. In the human middle-ear, the same function is performed by the bones *malleus, incus* and *stapes*, which are collectively known as the ossicles.

The extracolumella applies a significant mechanical load on the tympanum and thereby precludes its treatment as a freely vibrating membrane. Furthermore, the contact surface of the malleus on the human eardrum is more or less symmetric whereas the extracolumella is attached asymetrically.

For low frequencies (below 4kHz), the extracolumella vibrates as a completely stiff bar. It was shown by Manley [3] that the extracolumella begins to flex at higher frequencies - this is illustrated in fig. 2.3. This is partly responsible for the poor high-frequency response of gecko middle ears - a feature also observed in other non-mammalian verterbates. The reason for this is that, due to the flection some energy is lost and not transferred to the columella.

### 2.1.3 Head Model and External Sound Input

In realistic environments the acoustic fields experienced by animals are often very complex. In addition to sound waves radiated directly from one or more sources in general, they also involve waves reflected from objects in their immediate neighbourhood. Higher animals such as humans possess the neural power to carry out the sophisticated signal processing

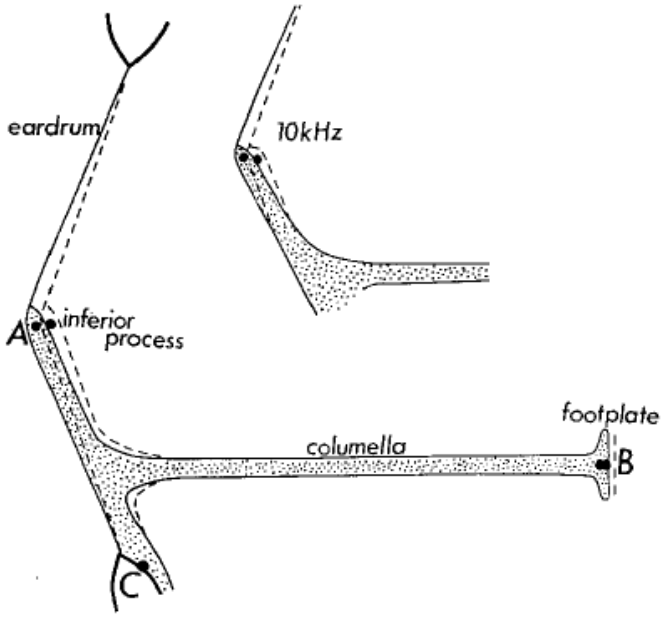


Figure 2.3: Operation of the middle ear lever in geckos reproduced from [3]. The inferior process of the extracolumella (A-C) hinges at point C at low frequencies. At high frequencies the inferior process flexes.

needed to derive useful information from these signals. Simpler animals like geckos respond to simpler cues - usually the direct field from the nearest or strongest source.

We can therefore model our incoming wave as the simple case of an incident plane wave of a certain frequency. This input is specified in terms of its intensity, frequency and direction. Such a stimulus can be generated in an anechoic chamber from loudspeakers which are placed at a distance from the animal that is large compared to the animal's size and the wavelength of the sound involved. Such experimental-setups are more thoroughly described by Christensen-Dalsgaard and Manley ([4], [5]) and Christensen-Dalsgaard, Tang and Carr ([6]).

The amplitude of the sound pressure incident on both ears can be taken as uniform in over the surface of the membrane. The spatial variation can be safely neglected because the typical eardrum is less than 5mm in diameter whereas the smallest sound wavelengths in the hearing range of the larger lizards (eg. Tokay gecko) is around 70mm (4000 Hz) and is around 50mm (7000 Hz) for the smaller lizards (eg. Hemidactylus). In other experiments, a similar stimulus has also been provided by means of a headphone sealed to the ear ([7]).

In general a the sound on the other side of the head will differ in phase as well as amplitude. This is a result of the diffraction of sound around the head and body of the animal. The exact variation depends on the size of the animal and the frequency of the incident wave. Due to the typically small head size of geckos, the amplitude variation (known as shadowing) is neglible. The phase difference, although small compared to those in larger animals, cannot be neglected. We therefore consider an incoming sound wave of

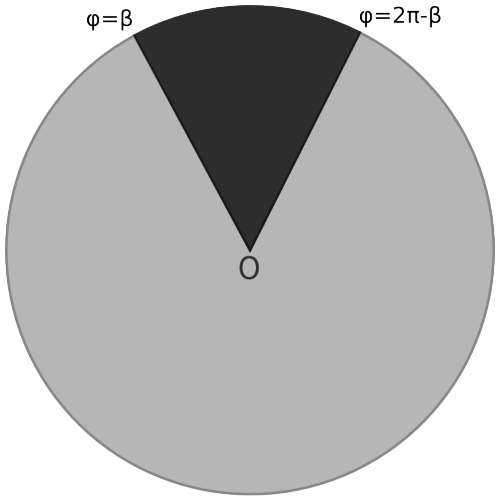


Figure 2.4: Model of the loaded tympanice membrane. The lightly shaded region is modelled as a linear elastic membrane whereas the darkly shaded region ($\beta < \phi < 2\pi - \beta$) represents the contact surface of the extracolumella and the membrane. $\beta$ is estimated from the anatomical data.

(pressure) amplitude $p$ and frequency $\omega$.

In the earlier ICE model, the effect of diffraction on the phase difference was neglected as well. The phase difference is found directly from the path difference $\Delta$ as shown in fig. 2.5. As a result, the sound pressure inputs at both ears is given by,

$$p_0 = pe^{j\omega t}e^{-k\Delta/2}, \qquad p_L = pe^{j\omega t}e^{k\Delta/2}, \qquad \Delta = L\sin\theta. \tag{2.2}$$

We note that in defining the input in this way, we've emphasized the symmetry of the system. We have chosen a coordinate system relative to the *median-sagittal* plane of the animal and $\theta$ gives the angle of incidence of this sound wave relative to this plane. For more complex auditory systems we would have requirde two angles $(\theta, \phi)$ to describe the three-dimensional system but in our analysis this is unnecessary.

The ear closer to the sound source is referred to as the *ipsilateral* ear and is denoted by a subscript 0 and the one further away from the source is referred to as the *contralateral* ear and is denoted by a subscript $L$. Subsequently, unless otherwise specified, the subscripts 0 and $L$ will correspond to the ipsi- and contralateral ears respectively.

## 2.2 Derivation of the Model

We will now use the previously described physical model to derive the main quantities of interest in the ICE model. We first find an expression for the pressure distribution in the cylindrical cavity and for the membrane vibrations subject to an external stimulus. We then apply the appropriate boundary conditions to relate the membrane vibrations to

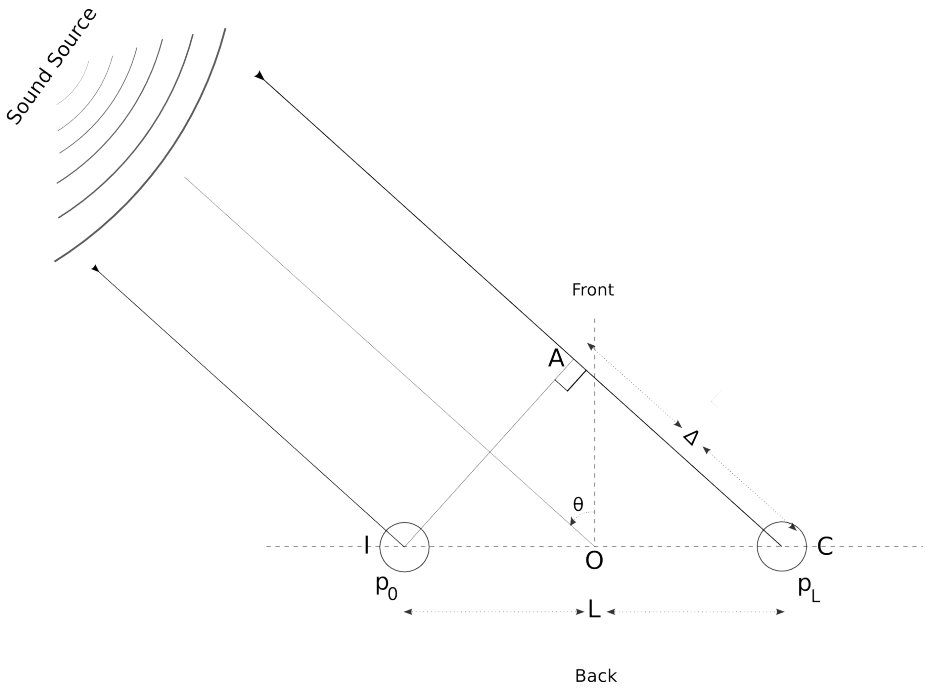


Figure 2.5: The previous acoustic head model for geckos. The extra distance travelled by the soundwave to reach the contralateral ear is denoted by $\Delta$.

the internal pressure and find the expression for the membrane vibrations as a function of direction and frequency.

### 2.2.1 Internal Cavity

We assume that the air inside the cavity obeys linear acoustics (briefly discussed in A). The pressure distribution inside the cavity is therefore given by the 3D acoustic wave-equation in cylindrical polar coordinates,

$$\frac{1}{c^2}\frac{\partial^2 p(x,r,\phi,t)}{\partial t^2} = \frac{1}{r}\frac{\partial}{\partial r}\left(r\frac{\partial p(x,r,\phi,t)}{\partial r}\right) + \frac{1}{r^2}\frac{\partial p(x,r,\phi,t)}{\partial \phi^2} + \frac{\partial p(x,r,\phi,t)}{\partial x^2} \tag{2.3}$$

where $c$ is the sound propagation velocity. The complete solution must take into account the boundary conditions at and within the cavity walls and the ones at the air-membrane interface. We also note that the above equation implies that the animal's mouth is closed, which is typical for a waiting animal. In order to solve (2.3) for a particular frequency $f$ (angular frequency $\omega = 2\pi f$), we use the following separation ansatz

$$p(x,r,\phi,t) = f(x)g(r)h(\phi)e^{j\omega t} \tag{2.4}$$

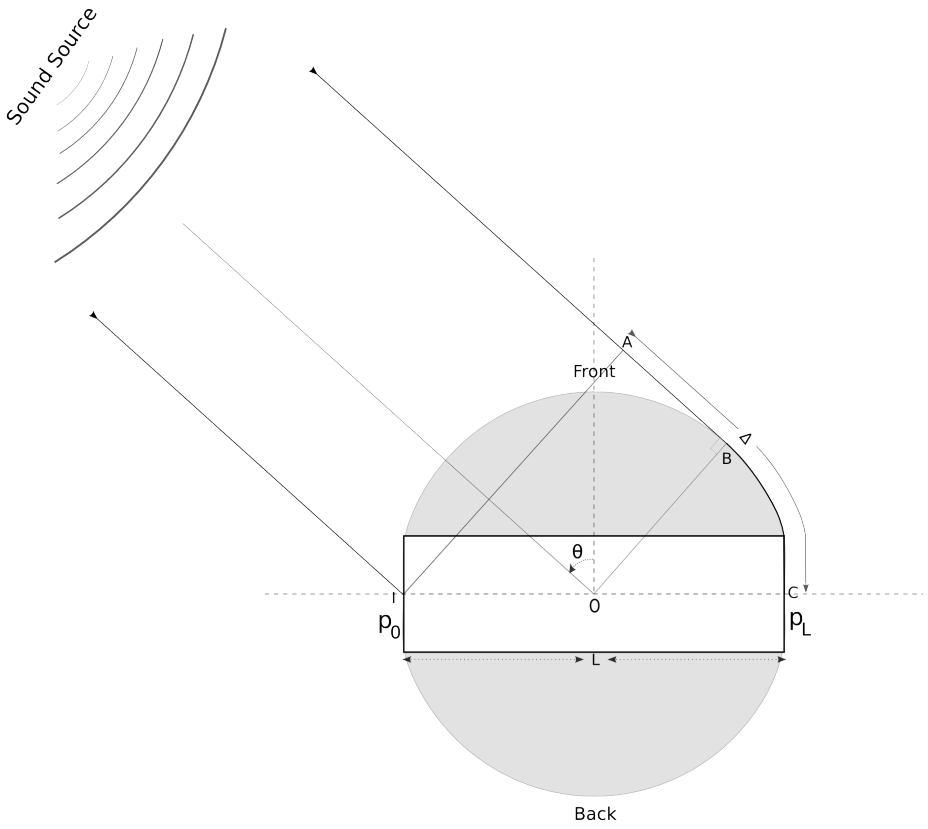


Figure 2.6: The acoustic head model for geckos. The white region is the internal cavity. As before, the extra distance travelled by the soundwave to reach the contralateral ear is given by $\Delta$.

which after substitution into the acoustic wave-equation leads to,

$$\begin{aligned} k^2 f(x)g(r)h(\phi) + f(x)h(\phi)\left[\frac{\partial^2 g(r)}{\partial r^2} + \frac{1}{r}\frac{\partial g(r)}{\partial r}\right] \\ + f(x)g(r)\frac{1}{r^2}\frac{\partial h(\phi)}{\partial \phi} + \frac{\partial^2 f(x)}{\partial x^2} = 0 \end{aligned} \tag{2.5}$$

with $k := \omega/c$. This results in the following set of separated ODE's,

$$\frac{d^2 f(x)}{dx^2} + \zeta^2 f(x) = 0 \tag{2.6}$$

$$\frac{d^2 h(\phi)}{d\phi^2} + q^2 h(\phi) = 0 \tag{2.7}$$

$$\frac{\partial^2 g(r)}{\partial r^2} + \frac{1}{r}\frac{\partial g(r)}{\partial r} + \left[\underbrace{(k^2 - \zeta^2)}_{=:\nu^2} - \frac{q^2}{r^2}\right] g(r) = 0 \tag{2.8}$$

with separation constants $q$ and $\zeta$. The last equation is the Bessel differential equation [8, p. 313] and its general solution is given by,

$$g(r) = C_{qs}J_q(\nu r) + D_{qs}Y_q(\nu r). \tag{2.9}$$

$J_q$ and $Y_q$ are the order-$q$ Bessel functions of the first and second kind respectively. The Bessel function of the second kind can be ignored as it diverges at $r = 0$. The solutions to the separated equations are therefore given by,

$$f(x) = e^{\pm\zeta x},\ h(\phi) = e^{\pm jq\phi}, \text{and } g(r) = J_q(\nu r) \tag{2.10}$$

with a specific solution to (2.3) given by,

$$p(x, r, \phi; t) = \left[(A^+e^{jq\phi} + A^-e^{-jq\phi})e^{j\zeta x} + (B^+e^{jq\phi} + B^-e^{-jq\phi})e^{-j\zeta x}\right] J_q(\nu r)e^{j\omega t}. \tag{2.11}$$

The coefficients $A^\pm$, $B^\pm$, $q$, $\zeta$ and $\nu$ will be subsequently determined by the boundary conditions.

In general, the time component of the pressure also has a *backward-moving* component, i.e. $e^{-j\omega t}$. By making the ansatz in (2.4), we have implicitly made use of the fact that the form of the input constrains the pressure to only have a *forward-moving* component, i.e. $e^{j\omega t}$.

### Pressure Boundary Conditions

There are three sets of boundary conditions -

- Continuity and smoothness in $\phi$ which is equivalent to $h(0) = h(2\pi)$ and $h'(0) = h'(2\pi)$ where, $h' = dh/d\phi$.
- Vanishing of the normal derivative at the cavity walls - $g'(a_C) = 0$ ($a_C$ is the radius of the cylinder).
- Equating the membrane velocity to the air velocity at the membrane boundaries (to be discussed in the next section).

The first set of requirements is obvious. This reduces (2.11) to

$$p(x, r, \phi; t) = \left[Ae^{j\zeta x} + Be^{-j\zeta x}\right] \cos q\phi J_q(\nu r)e^{j\omega t}. \tag{2.12}$$

With $q$ constrained to be an integer.

The second and third are a result of the so called "no-penetration" boundary-condition of fluid-mechanics. It arises from the from the fact that the cavity wall is an impermeable boundary. This translates into the requirement that the normal fluid-particle velocity should vanish ([9, p. 111]). The fluid-particle velocity ($\mathbf{v}$) is related to the pressure by,

$$-\rho\frac{\partial \mathbf{v}}{\partial t} = \nabla p \tag{2.13}$$

At the cylindrical cavity wall, the normal velocity is in the radial direction. Substituting the expression for pressure in (2.11) in the above equation leads to a Neumann boundary condition for the pressure,

$$\begin{aligned} v_r = -\frac{1}{j\rho\omega}\frac{\partial p(x,r,\phi;t)}{\partial r}\bigg|_{r=a_C} &= 0 \\ \Rightarrow \frac{\partial J_q(\nu r)}{\partial r}\bigg|_{r=a_C} &= 0 \end{aligned} \tag{2.14}$$

This constrains $\nu$ to a discrete set of values which correspond to the local minima and maxima of $J_q$. We can therefore index $\nu$ by $q$ and $s = 0, 1, 2, 3, \ldots$ with $\nu_{qs} = z_{qs}/a_C$: $z_{qs}$ being the $s^{th}$ extremum of the order-$q$ Bessel function of the first kind. This results in a discrete set of modes that satisfy (2.3) which are given by,

$$p_{qs}(x,r,\phi;t) = \left[A_{qs}e^{j\zeta_{qs}x} + B_q s e^{-j\zeta_{qs}x}\right] f_{qs}(r,\phi)e^{j\omega t} \tag{2.15}$$

where we have added the subscripts $q$ and $s$ to $\zeta$ and denoted the $(r,\phi)$ part of (2.12) by $f_{qs}(r,\phi)$. Effectively, the modes are 3D waves propagating with wave numbers $\zeta_{qs}$ in the $x$-direction and $\nu_{qs}$ in the radial direction. The first of these modes (corresponding to $q = 0, s = 0$) is of particular importance. Since the first maximum of $J_0$ occurs at $r = 0$, we have $\nu_{00} = 0$. This leads to the first mode being a plane-wave which is constant in $r$ and $\phi$ and only varies in $x$.

A very useful property of the above modes is their orthgonality, i.e.

$$\int_\Omega dV p_{q_1 s_1} p_{q_2 s_2} = 0, \; if \; q_1 \neq q_2 \; or \; s_1 \neq s_2 \tag{2.16}$$

the integral is over the volume of the cylinder. This is a consequence of the fact that for different $q$'s the cosine parts of the modes are orthogonal whereas for a given $q$ the Bessel parts are orthogonal for different $s$'s or expressed as an equation,

$$\int dS f_{q_1 s_1} f_{q_2 s_2} = 0, \; q_1 \neq q_2 \; or \; s_1 \neq s_2 \tag{2.17}$$

where $dS = r dr d\phi$ and the integral being taken over the disk of radius $a_C$. We can therefore write the general solution to (2.3) as a linear combination of the orthogonal modes given in (2.15),

$$p(x,r,\phi;t) = \sum_{q=0}^{\infty}\sum_{s=0}^{\infty}\left(A_{qs}e^{j\zeta_{qs}x} + B_{qs}e^{-j\zeta_{qs}x}\right) f_{qs}(r,\phi)e^{j\omega t} \tag{2.18}$$

The remaining coefficients, $A_{qs}$ and $B_{qs}$, will be determined by equating the fluid-particle velocity to the membrane velocity at both ends of the cylinder. To do so, we will first need to find an expression for the membrane vibrations and subsequently make use of some simplifying approximations.

### 2.2.2 Vibration of the Membrane

As a preliminary exercise, we will first derive expressions for the free and force-driven vibrations of a circular membrane. We will then use our results to move on to the sectoral membrane which corresponds to the tympanum loaded by the extracolumella. Thi corresponds to the approximating the extracolumella to have infinite mass.

#### Circular Membrane

The equation of motion for the vibration of a rigidly clamped circular membrane of radius $a_M$ solves for the membrane displacement $u$ at a point $(r, \phi)$ with $r < a$ and $0 < \phi < 2\pi$. It is given by,

$$-\frac{\partial^2 u(r,\phi;t)}{\partial t^2} - 2\alpha\frac{\partial u(r,\phi;t)}{\partial t} + c_M^2\left[\frac{1}{r}\frac{\partial}{\partial r}\left(r\frac{\partial u(r,\phi,t)}{\partial r}\right) + \frac{1}{r^2}\frac{\partial u(r,\phi,t)}{\partial \phi^2}\right] = \frac{1}{\rho_M d}\Psi(r,\phi;t) \tag{2.19}$$

subject to the boundary condition $u(r,\phi;t)|_{r=a_M} = 0$.. We've defined the following membrane material properties,

- $c_M$ - propagation speed of vibrations.
- $\alpha(> 0)$ - the damping coefficient.
- $\rho_M$ - density.
- $d$ - thickness.

$\Psi(r,\phi;t)$ is the pressure on the membrane surface at $(r,\phi)$. In our discussion we are only concerned with periodic and uniform pressure acting on the membrane surface. This is justified by the fact that for typical hearing ranges of these animals, the wavelength of sound is much greater than the membrane size and any spatial variation can be neglected.

#### Free Vibrations

**Undamped Membrane**: We first determine the eigenmodes of an undamped circular membrane by solving (2.19) for $\alpha = 0,\ \Psi = 0$. To do this we make a separation ansatz just as we did in (2.4),

$$u(r,\phi;t) = f(r)g(\phi)h(t) \tag{2.20}$$

This gives us the following set of equations

$$\frac{\partial^2 f(r)}{\partial r^2} + \frac{1}{r}\frac{\partial f(r)}{\partial r} + \left[\mu^2 - \frac{m^2}{r^2}\right] f(r) = 0 \tag{2.21}$$

$$\frac{d^2 g(\phi)}{d\phi^2} + m^2 g(\phi) = 0 \tag{2.22}$$

$$\frac{d^2 h(t)}{dt^2} + c_M^2\mu^2 h(t) = 0 \tag{2.23}$$

with separation constants $\mu$ and $m$. The solution of the first of these equations should already be familiar to us from the previous section - $J_m(\mu r)$, the order-$m$ Bessel function of the first kind. The boundary conditions in $\phi$ direction remain the same resulting in,

$$u(r,\phi;t) = \left[\left(M^+e^{jm\phi} + M^-e^{-jm\phi}\right)e^{jc_M\mu t} + (N^+e^{jm\phi} + N^-e^{-jm\phi})e^{-jc_M\mu t}\right]J_m(\mu r) \quad (2.24)$$

Unlike in the case of the internal cavity, we require $u$ to vanish at the boundary so we have a Dirichlet boundary condition which effectively requires: $J_m(\mu a_M) = 0$. This constrains $\mu$ to a discrete set of values which correspond to the zeros of $J_m$. The eigenmodes of a the circular membrane are therefore given by,

$$\begin{aligned} u_{mn}(r,\phi;t) = \left[(M^+_{mn}e^{jm\phi} + M^-_{mn}e^{-jm\phi})\,e^{j\omega_{mn}t} + \right. \\ \left. (N^+_{mn}e^{jm\phi} + N^-_{mn}e^{-jm\phi})e^{-j\omega_{mn}t}\right]\,J_m(\mu_{mn}r) \end{aligned} \quad (2.25)$$

where $\mu_{mn} = z_{mn}/a_M$, $z_{mn}$ being the $n^{th}$ zero of $J_m$ and, $\omega_{mn} = c_M\mu_{mn}$ is the eigenfrequency of the $(m,n)$ eigenmode. At this point $m$ can take any positive real value – a fact that will help us solve the sectoral membrane problem. However, in the case of a full circular membrane – as in the case of the pressure inside a cylindrical cavity – requirements of continuity and smoothness in $\phi$ reduce (2.25) to,

$$u_{mn}(r,\phi;t) = \cos m\phi J_m(\mu_{mn}r)\left[M_{mn}e^{j\omega_{mn}t} + N_{mn}e^{-j\omega_{mn}t}\right] \quad (2.26)$$

with $m = 0, 1, 2, \ldots$ with the $(m,n)$ eigenmodes forming an orthogonal set. For later convenience we denote the spatial part of the above mode by $u_{mn}(r,\phi)$. The first few of these modes are plotted in 2.7.

We note that unlike in the case of the internal cavity, the free membrane has components that are both forward- and backward-moving in time. The presence of a driving force, however, will result in simpler expressions. This will be discussed in more detail in the next chapter where we compare our model with experimental data.

**Damped Membrane**: For a damped membrane, i.e. $\alpha \neq 0$, the spatial part of the above eigenmodes remains the same. The form of the time-dependent part is given by the solution of the equation,

$$\frac{d^2h_{mn}(t)}{dt^2} + 2\alpha\frac{dh_{mn}(t)}{dt} + \omega^2_{mn}h_{mn}(t) = 0. \quad (2.27)$$

Assuming $h_{mn}$ takes the form $e^{j\widetilde{\omega}_{mn}}$ leads to a quadratic equation with solutions,

$$\widetilde{\omega}_{mn} = j\alpha \pm \omega^*_{mn} \quad (2.28)$$

$$\omega^*_{mn} = \sqrt{\alpha^2 + \omega^2_{mn}} \quad (2.29)$$

We require the membrane displacement to remain finite as $t \to \infty$. We can therefore neglect the $e^{-j\widetilde{\omega}_{mn}}$ terms leading to,

$$\widetilde{u}_{mn}(r,\phi;t) = \cos m\phi J_m(\mu_{mn}r)\left[M_{mn}e^{j\omega^*_{mn}t} + N_{mn}e^{-j\omega^*_{mn}t}\right]e^{-\alpha t} \quad (2.30)$$

The general solution is given by a linear combination of the above and the coefficients are determined by initial conditions – for example, membrane displacement and velocity at $t = 0$.

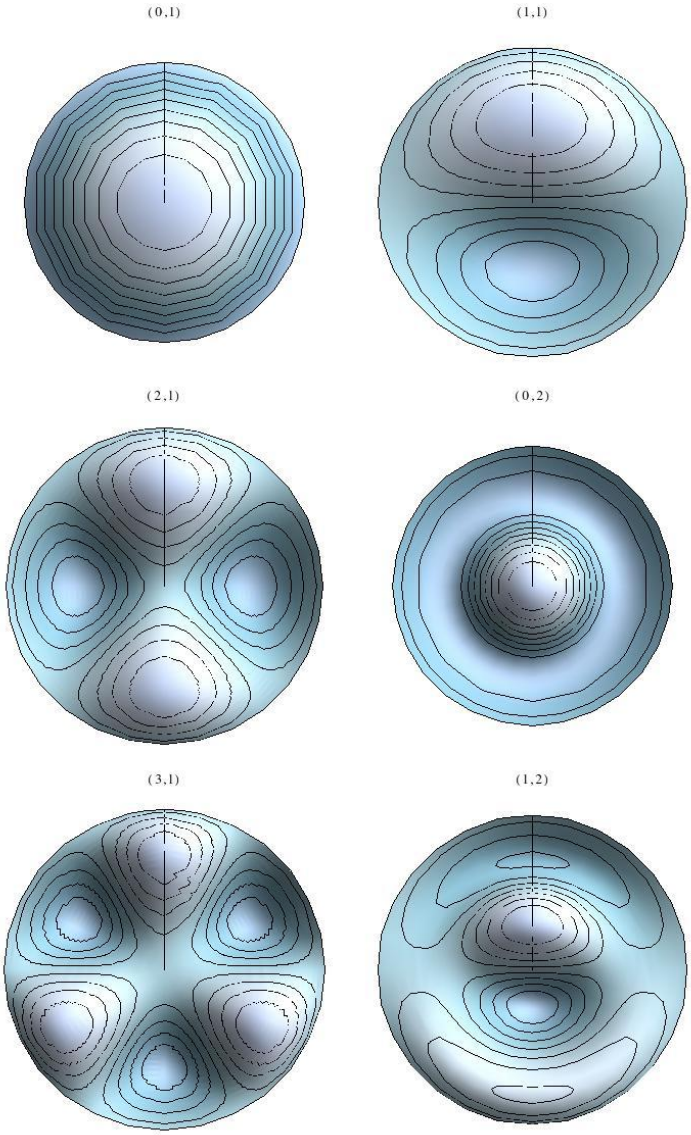


Figure 2.7: Eigenmodes of a full circular membrane. The eigenfrequency increases from left to right.

### Forced Vibrations

For a periodically driven membrane, there are two components of the full solution for forced vibrations. The first of these is the steady state solution which oscillates with the same frequency as the input and does not depend on the initial conditions - $u_{ss}$. The second of these is the transient solution that depends on the initial conditions but not on the driving pressure - $u_t$.

**Steady State Solution**: The steady state solution is expressed as a linear combination

of the spatial part of the above eigenmodes and is given by,

$$u_{ss}(r,\phi;t) = \sum_{m=0}^{\infty}\sum_{n=1}^{\infty} C_{mn}\cos m\phi J_m(\mu_{mn}r)e^{j\omega t}. \tag{2.31}$$

Substituting this expression in (2.19) with $\Psi = pe^{j\omega t}$ gives,

$$\sum_{m=0}^{\infty}\sum_{n=1}^{\infty} \Omega_{mn}C_{mn}\cos m\phi J_m(\mu_{mn}r)e^{j\omega t} = pe^{j\omega t} \tag{2.32}$$

$$\text{where, } \Omega_{mn} = \rho_M d(\omega^2 - 2j\alpha\omega - \omega_m^2 n). \tag{2.33}$$

Using the orthogonality of the eigenmodes, the coefficients $C_{mn}$ can be calculated,

$$C_{mn} = \frac{p\int dSu_{mn}}{\Omega_{mn}\int dSu_{mn}^2} \tag{2.34}$$

with the integral this time being taken over the circular disk of radius $a_M$.

**Transient Solution**: The transient solution is effectively a solution of the free damped membrane, i.e. a linear combination of the eigenmodes given in (2.30). Therefore,

$$u_t(r,\phi;t) = \sum_{m=0}^{\infty}\sum_{n=1}^{\infty} \cos m\phi J_m(\mu_{mn}r)\left[M_{mn}e^{j\omega^*_{mn}t} + N_{mn}e^{-j\omega^*_{mn}t}\right]e^{-\alpha t}. \tag{2.35}$$

The complete solution is given by $u = u_t + u_{ss}$ and the coefficients $M_{mn}$ and $N_{mn}$ are determined by the initial conditions (at $t = 0$).

**Steady State Approximation**: The damping coefficient $\alpha$ is usually given in terms of the membrane fundamental frequency and a quality factor $Q$ as $\alpha = \omega_{01}/2Q$. For the tympani we will be concerned with we have $Q \sim 1.2$ which results in damping coefficients that are around $4000s^{-1}$ for the larger lizards and around $8000s^{-1}$ for the smaller ones. Due to this and the exponential decay of the transient vibration amplitude, we can safely assume that within a few time-periods the steady-state vibrations dominate the solution of the forced membrane. For this reason, we will subsequently confine our discussion to only the steady state vibrations of the membrane.

### Sectoral Membrane

The eigenmodes of the sectoral membrane proceeds from (2.25) onwards. We now have a new set of boundary conditions in $\phi$. The extracolumella is modelled as a triangular plate of infinite mass which constrains the membrane displacement to go to zero at $phi = \beta$ and $\phi = 2\pi - \beta$. This results in the following set of eigenmodes,

$$u_{mn}(r,\phi;t) = \sin\kappa(\phi-\beta)J_\kappa(\mu_{mn}r)\left[M_{mn}e^{j\omega_{mn}t} + N_{mn}e^{-j\omega_{mn}t}\right] \tag{2.36}$$

where $\kappa[m] = \frac{m\pi}{2(\pi-\beta)}$, $m = 1, 2, 3, \ldots$. We see that the $r$ part of the above mode is given by the order-$\kappa$ Bessel function of the first kind; $\mu_{mn}$ being its $n^{th}$ zero, as before. The solution for the damped membrane follows in an identical way. It is apparent from the form of the above modes that, unlike in the case of the circular membrane eigenmodes, these modes are no longer circularly symmetric. We plot the first few of these modes in 2.8. The solution

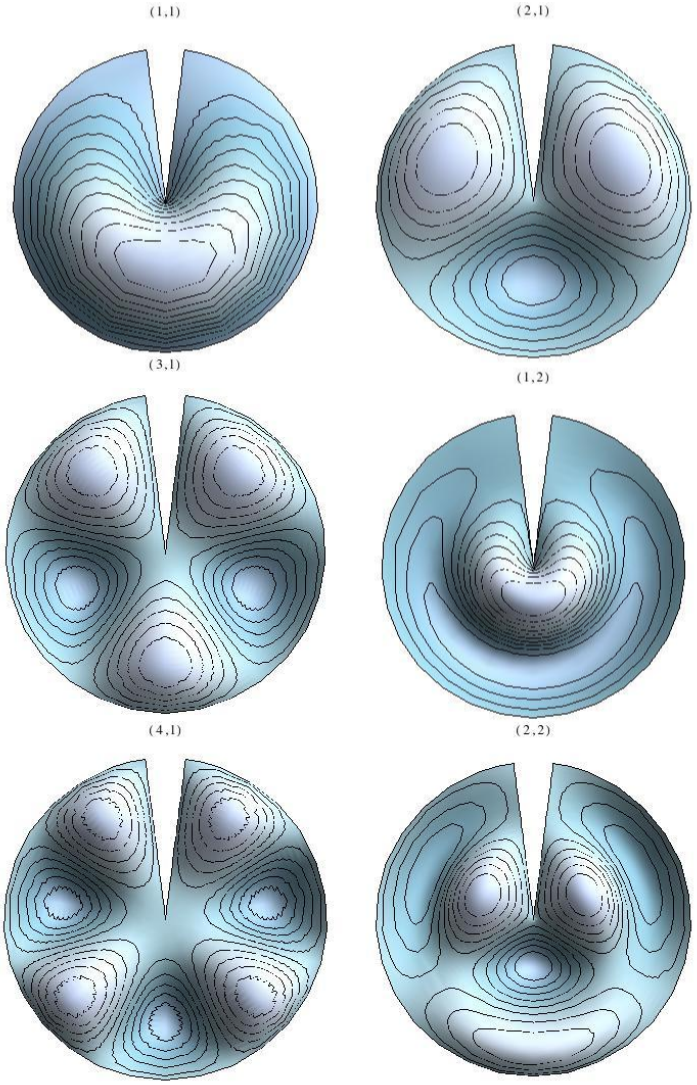


Figure 2.8: Eigenmodes of a sectoral membrane with $\beta = \pi/25$. The eigenfrequency increases from left to right.

for forced membrane vibrations follows in the same way as in the circular membrane case. The sectoral shape of the membrane has important physical consequences and captures the complex vibration patterns of a realistic membrane. This will be discussed in the next chapter.

### 2.2.3 Vibration of Coupled Membranes

With our current knowledge, we can move on to the main part of the chapter - the vibration of coupled membranes. It is convenient to first write down the main equations of the system based on our previously derived expressions. The vibrations of the membranes is given by,

$$u_{0/L}(r,\phi;t) = \sum_{m=0}^{\infty}\sum_{n=1}^{\infty} \Omega_{mn} C_{mn}^{0/L} u_{mn}(r,\phi) e^{j\omega t} = p_{0/L} e^{j\omega t} - p(0/L, r, \phi; t) \tag{2.37}$$

where 0 and $L$ denote the ipsi- and contra-lateral membranes respectively and the cavity pressure distribution, $p(x, r, \phi; t)$, is given by (2.18). The above equation is only valid on the membrane surface i.e., for $r < a_{tymp}$ and $\beta < \phi < 2\pi - \beta$.

As discussed in 2.2.1, the internal cavity pressure satisfies the no-penetration condition at solid boundaries. This means that at both ends of the cylinder, we equate the fluid particle velocity of air to the velocity of the membrane. We also note that since the membrane diameter is smaller than the cylinder diameter, we have to set the air-particle velocity to zero for $r > a_{tymp}$. Since the membrane displacement is only in the $x$-direction, we only need to calculate the same component of the velocity. Using the relation (2.13) we get,

$$v_x(x,r,\phi;t) = -\frac{1}{\rho\omega}\sum_{q=0}^{\infty}\sum_{s=0}^{\infty} \zeta_{qs}\left(A_{qs}e^{j\zeta_{qs}x} - B_{qs}e^{-j\zeta_{qs}x}\right) f_{qs}(r,\phi) e^{j\omega t} \tag{2.38}$$

and the exact boundary conditions are given by,

$$j\omega U_0 = v_x(0,r,\phi;t) \tag{2.39}$$

$$j\omega U_L = -v_x(L,r,\phi;t) \tag{2.40}$$

where we've used the direction conventions described in 2.1 and made the following definitions,

$$U_{0/L} = \begin{cases} u_{0/L},\ 0 < r < a_{tymp} \text{ and } \beta < \phi < 2\pi - \beta \\ 0, \text{ otherwise} \end{cases} \tag{2.41}$$

#### Plane Wave Approximation

As previously stated, the exact boundary condition would entail setting the air velocity to be exactly equal to the membrane displacement velocity. At this point, it is important to note that the internal cavity eigenmodes are not orthogonal to the membrane eigenmodes in general[1]. This means that every membrane eigenmode couples with every cavity eigenmode and that each of the coefficients $A_{qs}$ and $B_{qs}$ will be given by an infinite linear combination of the coefficients $C_{mn}^{0/L}$.

[1]This would also be true if we had full circular membranes on either end of the cylinder. Although, in this case we would have the added simplification that only the circularly symmetric cavity eigenmodes will be activated.

**Volume Displacement**: For later convenience, we also make the following definition for the volume displacement of the membrane

$$S_{0/L}(t) = \int dS u_{0/L}(r, \phi; t) \tag{2.42}$$

This is the integral over the membrane surface of the local displacement. Given the external parameters and boundary conditions, it only depends on time

# Chapter 3

# Analysis of the ICE–Model

## 3.1 Membrane Vibration Profile

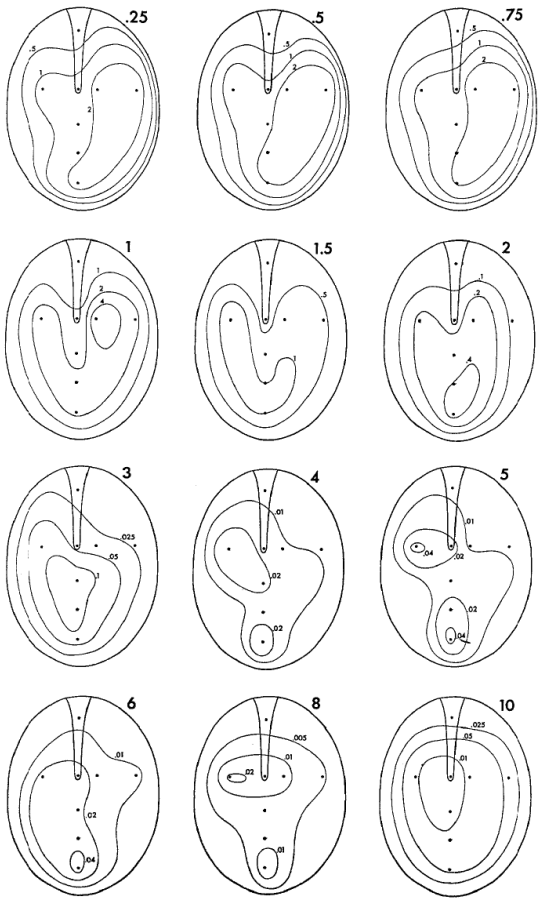


Figure 3.1: Experimental membrane vibration patterns of the Tokay gecko dependent on sound frequency (varying from .5kHz to 10kHz. Data taken from [10].

# Chapter 4

# Conclusion

# Appendix A

# Linear Acoustics

Hier steht der erste Anhang.

# Appendix B

# Second Appendix Chapter

Hier kommt der zweite Anhang.

# Bibliography


[1] C. Voßen, *Auditory Information Processing in Systems with Internally Coupled Ears*. PhD thesis, Technische Universität München, 2010.

[2] C. Voßen, J. Christensen-Dalsgaard, and J. L. van Hemmen, "Analytical model of internally coupled ears.," *Journal of the Acoustical Society of America*, vol. 128, pp. 909–918, 2010.

[3] G. Manley, "Frequency response of the middle ear of geckos," *Journal of comparative physiology*, vol. 81, no. 3, pp. 251–258, 1972.

[4] J. Christensen-Dalsgaard and G. A. Manley, "Directionality of the lizard ear," *J. Exp. Biol.*, vol. 208, pp. 1209–1217, Mar 2005.

[5] J. Christensen-Dalsgaard and G. Manley, "Acoustical coupling of lizard eardrums," *Journal of the Association for Research in Otolaryngology*, vol. 9, no. 4, pp. 407–416, 2008.

[6] J. Christensen-Dalsgaard, Y. Tang, and C. E. Carr, "Binaural processing by the gecko auditory periphery," *J. Neurophysiol.*, vol. 105, pp. 1992–2004, May 2011.

[7] C. Kppl and C. Carr, "Maps of interaural time difference in the chickens brainstem nucleus laminaris," *Biological Cybernetics*, vol. 98, no. 6, pp. 541–559, 2008.

[8] E. T. Copson, *Introduction to the Theory of Functions of a Complex Variable*. Oxford: Clarendon Press, 1973.

[9] C. Pozrikidis, *Fluid Dynamics: Theory, Computation, and Numerical Simulation*. Springer, 2009.

[10] G. A. Manley, "The middle ear of the tokay gecko," *Journal of Comparative Physiology*, vol. 81, no. 3, pp. 239–250, 1972.

# Acknowledgements

Danke.